

## BEAM DIAGNOSTIC SYSTEM FOR PAL-XFEL\*

J.Y. Huang<sup>#</sup>, H.S. Kang, S.J. Park, C.B. Kim, S.H. Jeong, S.H. Kim, Y.J. Park, S.C. Kim, M.H. Chun, Y.J. Han, I.S. Park, H.J. Park, D.T. Kim, S. Rah, J.H. Hong, Y.S. Bae, and I.S. Ko  
 Pohang Accelerator Laboratory, POSTECH, Pohang 790-784, Korea

### Abstract

Beam diagnostics for self amplification of spontaneous emission(SASE) x-ray free electron laser(XFEL) calls for precision of femto-second in time structure and sub-micrometer in beam position measurement. In the Pohang Accelerator Laboratory x-ray free electron laser (PAL-XFEL), thus, major development efforts should be performed on the measurement of femto-second bunch structure and sub-micrometer transverse beam position measurement techniques. The existing instruments can be used for standard diagnostics such as single bunch charge measurement, wire scanner or optical transition radiator for beam size measurement. Femto-second bunch length measurement can be realized using coherent transition radiation, and transverse deflecting cavity. Nanometer beam position measurement technique under development in collaboration with the linear collider group will be utilized for PAL-XFEL sub-micrometer beam position measurement. Overall plan and the ongoing development activities will be presented.

### INTRODUCTION

For the success of the proposed XFELs[1-5], the state-of-art electron beam quality is required. For the PAL-XFEL, it stands for low beam emittance ( $< 1 \mu\text{m}\cdot\text{rad}$ ), ultra-short bunch length (25  $\mu\text{m}$ ~80 fs), high peak current(~3.5 kA), high stability of beam energy ( $< 0.01 \%$ ) for the linac electron beam, and measurement and steering of beam trajectory within few micrometers ( $< 2 \mu\text{m}$ ) [6]. Typical layout and beam parameters for a proposed PAL-XFEL are shown and listed in Fig. 1 and Table 1 respectively.

Table 1: Beam parameters related to XFEL diagnostics

	Injector	BC1	BC2	undulator
beam energy	140 MeV	450 MeV	800 MeV	3.7 GeV
bunch charge	1.0 nC	1.0 nC	1.0 nC	1.0nC
bunch length (rms)	900 $\mu\text{m}$ (3 ps)	110 $\mu\text{m}$ (300 fs)	25 $\mu\text{m}$ (80 fs)	25 $\mu\text{m}$ (80 fs)
peak current	0.1 kA	1 kA	3.5 kA	3.5 kA
beam size ( $\sigma_x, \sigma_y$ ) $\mu\text{m}$	(135, 125)	(115, 100)	(68, 62)	(68, 62)
beam emittance	1.0 $\mu\text{mrad}$	1.0 $\mu\text{mrad}$	~1.0 $\mu\text{mrad}$	~1.0 $\mu\text{mrad}$
energy spread	$\sim 10^{-4}$	$\sim 10^{-4}$	$\sim 10^{-4}$	$\sim 10^{-4}$

Consequently, more accurate, high resolution and reliable beam diagnostic technology is required for the PAL-XFEL than the existing techniques used for the third generation light sources like Pohang Light Source(PLS). We need bunch-by-bunch measurements of electron and photon beam parameters at critical locations along the beam injector, bunch compressor, linac and undulator to verify, control and feedback machine components for the optimal tuning of XFEL. Major beam parameters to be measured for proposed PAL-XFEL will be:

- beam position with 10  $\mu\text{m}$  resolution in the Linac
- bunch length with 10 fs resolution
- electron beam profile and size with 5  $\mu\text{m}$  resolution
- beam emittance with 10% accuracy
- bunch charge with pico-Coulomb accuracy
- beam energy and energy spread with 0.01% accuracy
- beam position in undulator with 2  $\mu\text{m}$  resolution
- radiation intensity in the undulator with 1% accuracy

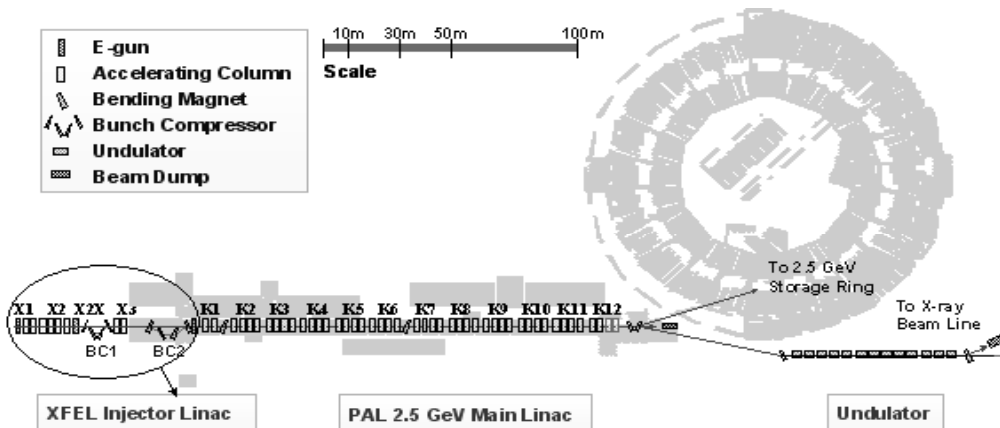


Fig. 1: Layout of PAL-XFEL rendered over existing 2.5GeV Linac and storage ring synchrotron radiation facility.

\*Work supported by POSCO and MOST

<sup>#</sup>huang@postech.ac.kr

As the conventional beam diagnostic technology has been well developed through the construction and operation of PLS, major researches for PAL-XFEL diagnostics will be focused on the single pass beam position measurement with sub-micrometer resolution, femto-second bunch length measurement techniques, and the photon beam diagnostic techniques along the undulator. Locations and related instruments of the beam diagnostic system are summarized in Table 2.

Table 2: Diagnostic systems: locations and instruments

Diagnostic parameters	Location	Related instruments
Bunch length (> 1 ps)	Injector before BC1	Streak Camera
Bunch length (< 1 ps)	after BC1(CSR) after BC2(EO) end of Linac(rf) end of undulator(CSR)	Coherent Synch. Radiation(CSR) Electro-Optic crystal rf deflector
Beam profile	Distributed over Linac and Undulator	OTR SR(interferometry) Wire scanner(WS)
Beam emittance	Injector, After BC1, BC2 End of Linac	OTR/WS +FODO transport
Slice emittance	After BC1, BC2, End of Linac	0-phasing+analysing station + OTR
Bunch charge	Distributed over Linac and Undulator	Integrating Current Transformer(ICT)
Beam energy and energy spread	BC1, BC2 End of Linac End of Undulator	(dispersion) + OTR (+analysing station)
Beam position monitor	Distributed over Linac and Undulator	Stripline BPM Cavity BPM
x-ray intensity	Along Undulator	Crystal diffractor + PIN diode detector

- OTR: Optical Transition Radiation
- CTR/CDR: Coherent Transition/Diffraction Radiation
- SR: Synchrotron Radiation

## BEAM POSITION MONITOR

Preservation of the beam quality during the beam transport and lasing of the XFEL radiation along the undulator are guaranteed only when the electron beam trajectory is well aligned within the specified tolerance, that is about 10% of the beam size. In PAL-XFEL, it should be tighter because of the low energy (3.7 GeV) and very narrow gap (~3 mm) in-vacuum undulator. Beam trajectory has to be maintained within 10  $\mu\text{m}$  in the linear accelerator and within 2  $\mu\text{m}$  in the undulator line.

The transverse position of the beam in the XFEL can be measured using two different types of beam position monitors. A sketch of a stripline BPM is shown in Fig. 2a. When each stripline covers the angle  $\phi$  of the beam pipe of the radius  $R$  and the electron beam is positioned on  $(x, y)$ , the electric signal  $V(x, y)$  induced on the stripline can be approximated as  $V(x, y) \sim \tan^{-1} [((R+x)^2+y^2)\tan(\phi/4) - 2yR]/(R^2-x^2-y^2)$  using the image charge method. To see a sensitivity behaviour, a beam current-independent x-axis

sensitivity  $S(x) = S(x,0) = V(x,0)/V(-x,0)$  is shown in Fig. 2b, where  $S(X) \sim \tan^{-1}[(1+X)\tan(\phi/4)/(1-X)] / \tan^{-1} [(1-X)\tan(\phi/4)/(1+X)]$  with a normalized position  $X = x/R$ .

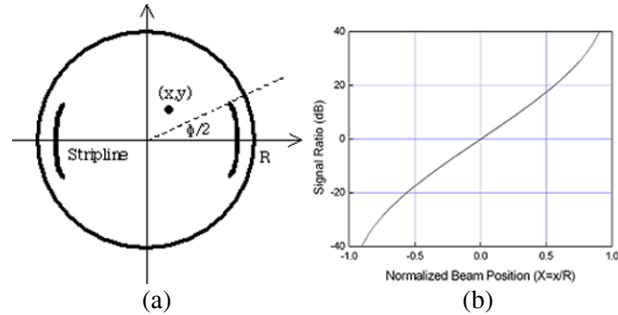


Fig. 2: (a) Schematic sectional view of a stripline and, (b) the sensitivity plot for  $S(x)$ .

In the undulator line, because of the tighter resolution requirements, cavity BPMs will be used together with stripline BPM. Cavity BPM has been intensively studied for nanometer beam position measurement for the future International Linear Collider(ILC).[8] In a cavity BPM, the amplitude of the TM<sub>110</sub>-mode, excited in the cavity by an off-centered beam, yields a signal proportional to the beam displacement and the bunch charge. For a pillbox cavity like Fig. 3a, the maximum TM<sub>110</sub> signal  $V_{110}(x)$  will be  $V_{110}(x) = 2k_{110}QJ_1(a_{11}x/r)/J_1^{\max}$ , where  $k_{110} = (\omega/2)(R/Q)_{110}$ ,  $a_{11}$  is the first root of  $J_1$ , and  $J_1^{\max} \sim 0.582$ , and  $R/Q$  is the cavity constant.[9] For a typical size of cavity BPM( $r \sim 100\text{mm}$ ),  $V_{110}(x)$  is about 10mV/ $\mu\text{m}$  at center with 1nC bunch. Sub-micrometer resolution of the cavity BPM can be achievable, although the measurable range of the cavity BPM is very narrow, typically less than 500  $\mu\text{m}$ . Figure 3b shows a sensitivity map obtained from model cavity BPM parameters.

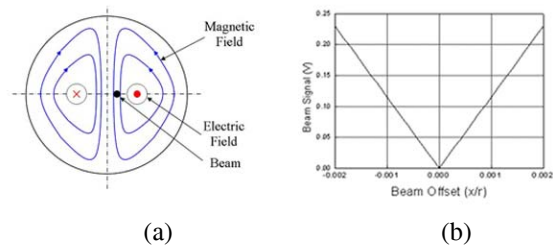


Fig. 3: (a) Typical TM<sub>110</sub>-mode excited by off-centered beam in cavity BPM and (b) a response near the center.

## BUNCH LENGTH MEASUREMENT

In the PAL-XFEL, the electron bunch length at the photocathode will be around 10 ps, but rapidly decrease to shorter bunch by the end of focusing solenoid coils. After the first accelerating column, it is compressed down to around 3 ps. It is further compressed in the first bunch compressor (BC1) to 300 fs and finally shortened to

around 80 fs (25  $\mu\text{m}$ ) after the second bunch compressor (BC2)[5,10]. As the bunch length varies along the accelerator components, appropriate kind of bunch length measurement tool should be selected. Commercial streak cameras, such as Hamamatsu Fesca streak camera [11], are useful instrument for the measurement of spatio-temporal structure of electron bunch longer than 200 fs. Synchrotron radiation or optical transition radiation(OTR) [12] can be used for the direct bunch length measurement using streak camera. Since the resolution of the streak camera is limited to around 200 fs [11], alternate methods for bunch measurement should be used after the first bunch compressor. Autocorrelation of coherent synchrotron radiation (CSR) from a dipole magnet or coherent transition radiation (CTR) from a metal foil target can be used for the bunch length measurement. [13] When the micro-bunching instability grows, the CSR or CTR amplitude increases quadratically in the spectrum with respect to bunch charge. This characteristic can be utilized as an on-line bunch length monitoring-device during the operation.

For the time-domain sub-picosecond bunch length diagnostics, transverse rf deflecting cavity will be used. Fig.4 shows the principle of transverse rf deflector developed in SLAC [14]. The rf deflector generates transverse electric field to accelerate the beam in vertical direction while the beam passes through the deflector cavity. At the OTR target, bunch length  $\sigma_z$  converts to height of the image as  $\sigma_z \sim \lambda_{\text{rf}} E [(\sigma_y^2 - \sigma_{y0}^2) / \beta_d \beta_s]^{1/2} / 2\pi [eV_0 \sin \Delta \psi \cos \Theta]$ , where  $(\sigma_y, \sigma_{y0})$  are beam sizes measured with rf deflector (ON, OFF),  $E$  is beam energy,  $(\beta_d, \beta_s)$  are betatron functions at rf deflector and OTR foil,  $\lambda_{\text{rf}}$  and  $V_0$  are rf wavelength and voltage, and  $\Theta$  is rf phase.[15] This kind of rf deflector is applied for the diagnostics of sub-picosecond bunch length in TTF [2].

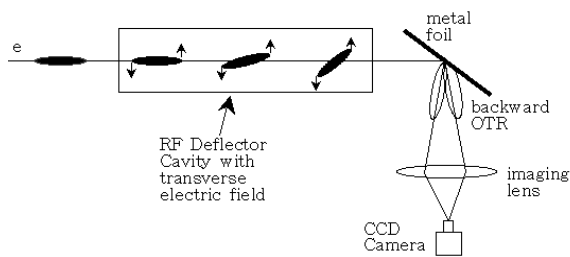


Fig.4: Conceptual rendering of rf deflector and OTR

Recent progress on the electro-optical (EO) bunch measurement technology using electro-optic crystals like  $\text{LiNbO}_3$ ,  $\text{TiNbO}_3$ ,  $\text{ZnTe}$  demonstrated very promising [16]. As the electric field of relativistic bunch propagates parallel with electron bunch, high electric field from electron bunch modifies refractive index of the EO crystal. Bunch structure can thus be detected with a polarized laser as a probe pulse, and detecting the modification of polarization during the laser beam passes through the EO crystal, as shown in Fig. 5. Although this technology has limited resolution by the dispersion of the laser light

through the EO crystal, bunch by bunch single shot measurement is possible as it does not intercept the beam.

EO detected signal of the beam is very important timing signal in synchronization of electron beam, laser light and FEL radiation within a few femto-second precision.[17] Fine improvement of electro-optic measurement technique is one of the major research activities in the FEL diagnostics.

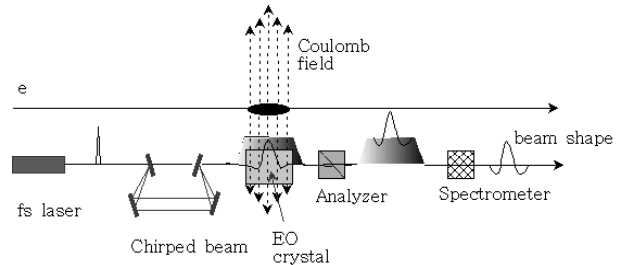


Fig. 5: fs bunch measurement using chirped laser pulse and EO crystal.

## BEAM PROFILE AND EMITTANCE

XFEL beam emittance should satisfy the diffraction limited beam relation  $\varepsilon \sim \sigma \sigma' < \lambda / 4\pi$  ( $\sigma$ ; beam size,  $\sigma'$ : beam divergence)[18]. Accurate beam emittance measurement is correlated with accurate measurement of beam size. Optical transition radiation, that is produced when a charged particle passes through a boundary of two media having different dielectric constant, can be used for the projected beam size measurement. The synchrotron radiation (SR) from a dipole magnet can be used for the beam size measurement by double-slit interferometry[19]. Since the transverse coherence at fixed wavelength becomes better as the beam size becomes smaller, measurement accuracy of the stellar interferometry will be  $\delta \sim |L/D|\lambda$  ( $L$ : source to slit distance,  $D$ : slit spacing)[19]. Better than  $3\mu\text{m}$  accuracy is possible with visible light.

Beam emittance can be measured with OTR screen and a quadrupole magnet located at non-dispersive section ( $\varepsilon \beta)(D\delta)^2$ ) as shown in Fig. 4. Using transport matrix  $R$ , beam size  $\sigma_2$  can be written as  $\sigma_2^2 = \varepsilon \beta_2 = \varepsilon (R_{11}^2 \beta_1 - 2R_{11}R_{12} \alpha_1 + R_{12}^2 \gamma_1)$  [20]. With quadrupole strength  $k$  and drift space  $L$ ,  $R_{11} = 1 + Lk$ ,  $R_{12} = L$ , and  $\sigma_2 \sim \varepsilon (Lk)^2 \beta_1$ . For the practical reason that quadrupole scanning method takes a long time, we will use four screens installed in a FODO lattice section to avoid changing quadrupole strengths.

Since the XFEL performance depends on slice emittance of the bunch, it is very important to have measurement capability of slice beam profile along the bunch. Slice emittance can be measured by combining rf-deflector and OTR beam size measurement system. Similarly, slice beam profile can be measured by zero-phasing the accelerating column and passing the electron beam through an analyzing magnet [21]. As the energy is modified linearly along bunch length, each slice of electron bunch makes image on the OTR screen.

## BUNCH CHARGE

An integrating current transformer can be used for the bunch by bunch charge measurement. At the low energy part of the linac, Faraday cup is used for the charge measurement and beam-dump as well. In the linac section, commercial integrating current transformer (e.g., Bergoz ICT) will be used. It measures bunch-by-bunch charge with 5 pC accuracy in measurable range of 2 nC. For some non-critical applications, sum signals from each BPM can be used for the bunch charge measurement with appropriate calibrations.

## BEAM ENERGY AND ENERGY SPREAD

Small change of beam position  $\Delta x$  is proportional to the change of beam energy at dispersive section with dispersion function  $\eta$ , as  $\Delta x \sim \eta(\Delta E/E)$ . Thus the beam energy variation can be monitored with an OTR screen at the dispersive section. Larger OTR screen will be needed at the low energy dispersive part like BC1, since the spread of beam image will be large in the dipole magnets at low energy. As the XFEL performance depends on the slice parameters, slice energy spread measurement is also very important. Slice energy spread can be measured by bending the rf-deflected bunch in the perpendicular direction with analysing magnet. Separate beam analyzing stations will be installed for the beam energy and spread measurements during the machine operation.

## UNDULATOR RADIATION

When the linac beam quality meets stringent XFEL requirements, it will radiate and amplify the synchrotron radiation along the undulator.[22] When undulator parameters satisfy the condition  $\lambda = \lambda_u(1 + a_u^2 + \gamma^2 \Theta^2)/2\gamma^2$  ( $\lambda_u$ : undulator period,  $a_u$ : undulator parameter,  $\Theta$ : radiating angle), FEL radiation is amplified through the interaction between bunched electron beam and synchrotron radiation along the undulator line as  $P \sim P_0 \exp(L/L_G)$ , where  $L_G$  is the gain length.[22] Important undulator parameters such as gain length and intensity of x-ray have to be measured along the undulator also. Thus beam diagnostics along the undulator includes beam position monitors, bunch charge monitors, beam profile monitors and x-ray intensity monitor. FEL intensity can be measured using a photon beam pick-up crystal and semiconductor detectors with a setup like in Fig. 6. As the XFEL radiation is not available, but under development, variety of ideas are proposed and being studied for characterization of XFEL radiation.[1, 4]

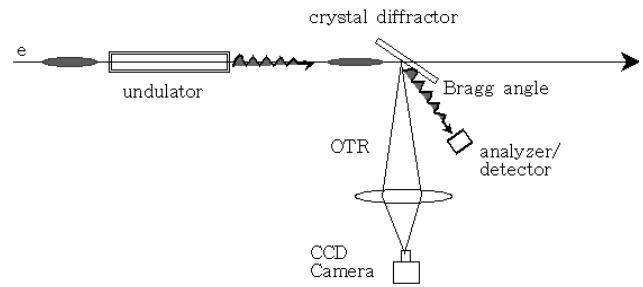


Fig. 6: Setup of FEL radiation monitor in the undulator using crystal diffractor.

## SUMMARY

General descriptions on the special diagnostic techniques for the proposed PAL-XFEL have been introduced. Further studies are still ongoing for the reliable and accurate measurements of sub-micrometer beam position measurement and sub-picosecond bunch length measurements. Further details of the design and implementation of the XFEL beam diagnostic systems can be found in the cited references.

## REFERENCES

- [1] LCLS Conceptual Design Report, SLAC-R-593, 2002
- [2] TTF Design Report, ed. by D. A. Edwards, 1995.
- [3] SCSX XFEL Conceptual Design Report, 2005.
- [4] BESSY Soft X-ray Free Electron Laser Technical Design Report, 2004.
- [5] PAL-XFEL Conceptual Design Study, to be published.
- [6] Y. Kim et. al., Proc. of 2004 FEL Conference, 2004.
- [7] T. Kamps, TESLA-FEL 2000-01.
- [8] Marc Ross et. al., SLAC-PUB-9887, 2003.
- [9] C. Magne, M. Wendt, DESY-TESLA-2000-41.
- [10] T. Raubenheimer, P. Emma, S. Kheifets, Proc. of PAC93, p635 (1993).
- [11] Hamamatsu FESCA-200 (C6138) has 200 fs-rms single-shot resolution
- [12] D. W. Rule, Nucl. Instrum. Meth. **B24**, 901 (1987).
- [13] U. Happek, A. Sievers, E. Blum, Physical Review Letters **67**, 2962(1991).
- [14] O. H. Altenmueller, R. R. Larsen, G. A. Loew, SLAC-PUB-17, 1963.
- [15] R. Akre, et. al, Proc. of EPAC02, p1882(2002).
- [16] G. Berden et. al, Phys. Rev. Lett. **93**, 114802(2004).
- [17] A. Cavalieri, et. al, Phys. Rev. Lett. **94**, 114801(2005).
- [18] K. J. Kim, Nucl. Instrum. Methods, **A261**, 44(1987).
- [19] T. Mitsuhashi, Proc. of PAC97, p766(1997).
- [20] M.C. Ross, et. al., Proc. of PAC87, p728(1987).
- [21] W. S. Graves, et. al., Proc. of PAC01, p2224 (2001).
- [22] J. B. Murphy and C. Pellegrini, *Laser Handbook*, North-Holland, pp9-70 (1990).